Analyst

www.rsc.org/analyst

Volume 137 | Number 14 | 21 July 2012 | Pages 3181–3392

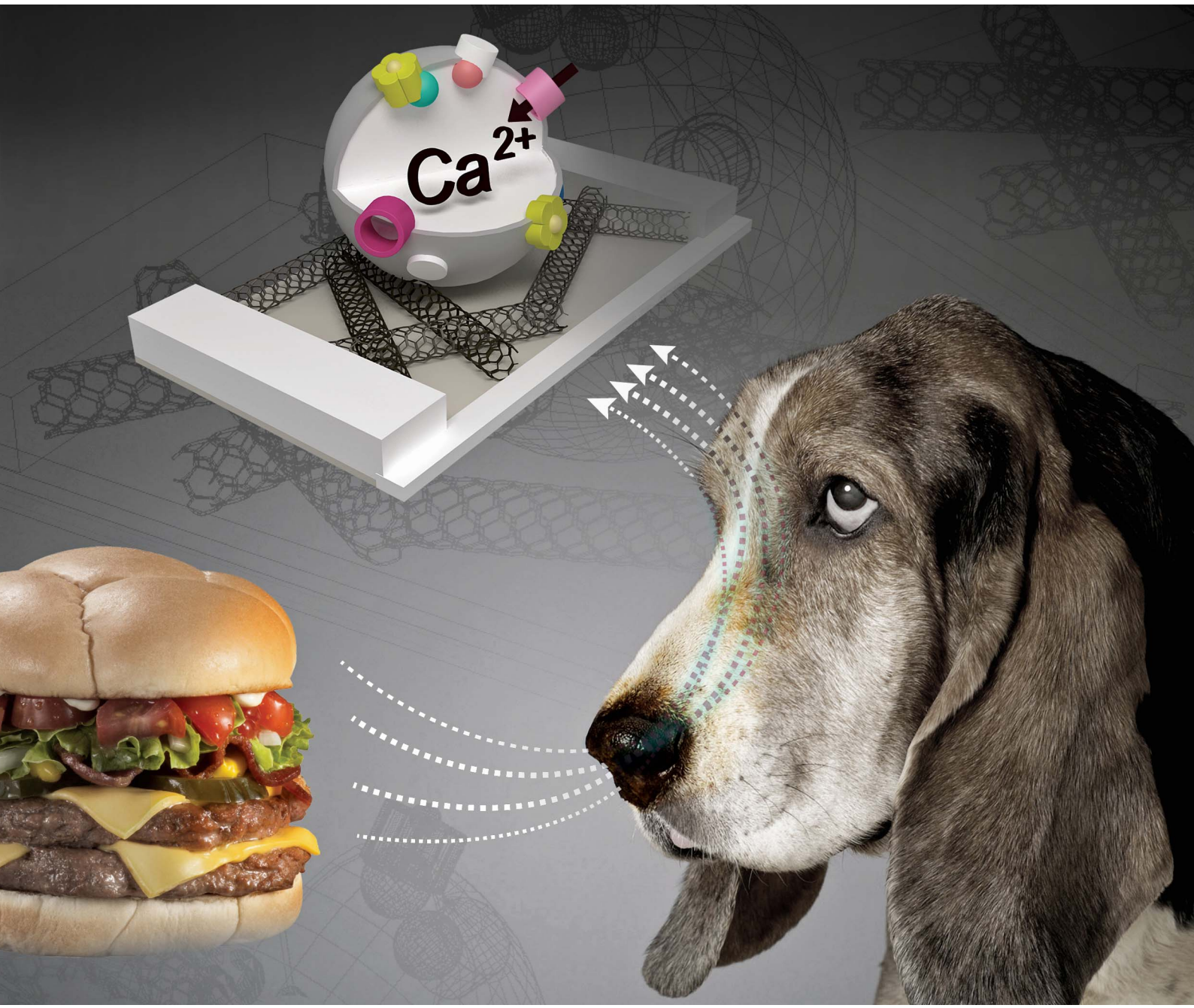

ISSN 0003-2654

HOT ARTICLE

Tai Hyun Park, Seunghun Hong *et al.*,
A bioelectronic sensor based on canine olfactory nanovesicle–carbon nanotube hybrid structures for the fast assessment of food quality

RSC Publishing

0003-2654(2012)137:14;1-2

Analyst

Dynamic Article Links

Cite this: *Analyst*, 2012, **137**, 3249

www.rsc.org/analyst

PAPER

A bioelectronic sensor based on canine olfactory nanovesicle–carbon nanotube hybrid structures for the fast assessment of food quality†

Juhun Park,‡[a] Jong Hyun Lim,‡[b] Hye Jun Jin,[a] Seon Namgung,[a] Sang Hun Lee,[b] Tai Hyun Park*[b] and Seunghun Hong*[ac]

Received 19th December 2011, Accepted 2nd March 2012
DOI: 10.1039/c2an16274a

We developed an olfactory-nanovesicle-fused carbon-nanotube-transistor biosensor (OCB) that mimics the responses of a canine nose for the sensitive and selective detection of hexanal, an indicator of the oxidation of food. OCBs allowed us to detect hexanal down to 1 fM concentration in real-time. Significantly, we demonstrated the detection of hexanal with an excellent selectivity capable of discriminating hexanal from analogous compounds such as pentanal, heptanal, and octanal. Furthermore, we successfully detected hexanal in spoiled milk without any pretreatment processes. Considering these results, our sensor platform should offer a new method for the assessment of food quality and contribute to the development of portable sensing devices.

Introduction

With growing interest in food safety, effective sensor platforms for the easy and fast on-site assessment of food quality have been drawing huge attention. Since various volatile compounds are produced in the process of the oxidation of food, the detection of such volatile compounds can be an effective strategy.[1–6] Typically, analytical methods such as gas chromatography-mass spectroscopy and high-performance liquid chromatography have been used for the detection of the volatile compounds.[1,7–9] However, those methods are not suitable for the on-site assessment of food quality due to their complicated pretreatment processes, a long measurement time, and laborious manipulations. Furthermore, the large sized equipment for chromatographic methods is a major obstacle to the development of portable sensors. As alternatives, semiconductor-based sensors have been studied extensively.[10–12] However, the capability of those devices is still inferior to that of the animal olfactory system in terms of its selectivity and sensitivity.

In the animal olfactory system, specific odorants bind to corresponding olfactory receptors (ORs) with high selectivity.[13–15] After the binding of odorants to ORs, a chemical signal is generated. The generated signal is converted into an electrical signal and amplified through a signaling pathway in an olfactory sensory neuron. Using this mechanism, animals can recognize odorants with high selectivity and sensitivity. To take advantages of the high sensitivity and selectivity of animal olfactory systems, many researchers have developed various strategies such as olfactory cell-based sensors and OR protein-based sensors.[16–20] However, since such sensors did not use the signaling pathway of the animal olfactory system, they had limitations in mimicking the high sensitivity of the animal olfactory system.

Herein, we report an olfactory-nanovesicle-fused carbon-nanotube-transistor biosensor (OCB) that mimics canine nose responses for the sensitive and selective detection of hexanal, an indicator of the oxidation of food. In this method, we prepared nanovesicles including canine ORs (cfOR5269), specific receptors for hexanal, and fixed them on a CNT channel in a CNT transistor to build an OCB. And then, the binding of hexanal to the cfOR5269 on the nanovesicles was detected by measuring the conductance change of the CNT channel.[15] We demonstrated the detection of hexanal at 1 fM concentration in real-time. Significantly, OCBs could selectively detect hexanal with an excellent selectivity capable of discriminating hexanal from analogous compounds such as pentanal, heptanal, and octanal. Furthermore, we could detect hexanal in spoiled milk without any pretreatment processes. OCBs can be an ideal strategy in building a portable electronic device for the easy and fast assessment of food quality.

Experimental

Production of canine olfactory nanovesicles

Human embryonic kidney (HEK)-293 cells were cultured in Dulbecco's modified Eagle's medium (DMEM; WelGENE, South Korea) containing 10% fetal bovine serum (FBS, Gibco,

[a]*Department of Physics and Astronomy, Seoul National University, Seoul, 151-742, Korea*
[b]*School of Chemical and Biological Engineering, Bio-MAX Institute, Seoul National University, Seoul, 151-742, Korea. E-mail: thpark@snu.ac.kr*
[c]*Department of Biophysics and Chemical Biology, Seoul National University, Seoul, 151-742, Korea. E-mail: seunghun@snu.ac.kr*

† Electronic supplementary information (ESI) available: Experimental procedure and supplementary figures. See DOI: 10.1039/c2an16274a

‡ These authors contributed equally to this work.

USA) and 1% penicillin–streptomycin (PS, Gibco, USA) at 37 °C in a 5% CO_2 environment (Fig. S1 in the ESI†). The cells (>90% confluent) were transfected with 4 μg of pIRES plasmids encoding influenza virus leader peptide, myelocytomatosis cellular oncogene (cMyc) epitope-tag, and cfOR5269 (received from Prof. Francis Galibert) using Lipofectamine2000 reagent (Invitrogen, USA) according to the manufacturer's protocol. The influenza virus leader peptide and the cMyc tag were incorporated to assist the membrane localization and the immunoblotting of cfOR5269, respectively. And, the transfected cells were subsequently cultivated again for 48 h. Nanovesicles with cfOR5269 were produced from the cfOR5269-expressed cells by incubating the cells with agitation in serum-free DMEM containing cytochalasin B (10 μg mL^{-1}, Sigma, USA) at 37 °C for 25 min. Here, the nanovesicles were separated from the cells by centrifugation at 500*g* for 10 min in an Eppendorf tube and then collected by centrifugation at 15 000*g* for 30 min. The nanovesicles were finally resuspended in Dulbecco's phosphate buffered saline (DPBS, Gibco, USA) with 1000 ng mL^{-1} of total protein density.[21] The prepared nanovesicles could be kept frozen below −70 °C for a long time period just like cells, and they were melted right before the fabrication of our OCB devices.

Immunoblot analysis

Nanovesicles with cfOR5269 were lysed by sonication for 5 min, and proteins in the nanovesicles were separated by sodium dodecyl sulfate-polyacrylamide gel electrophoresis. The proteins on the gel were transferred to a polyvinylidene fluoride membrane (PVDF, Bio-Rad, USA) under a constant current setting of 0.12 A for 90 min. The membrane was incubated in blocking solution (5 wt% skim milk in PBS containing 0.1 vol% Tween-20) at 25 °C for 2 h. The blocked membrane was incubated in the solution of anti-cMyc mouse antibody (1 : 1000 dilution in PBS-Tween, Santa Cruz Biotechnology, USA) at 25 °C for 2 h. Then, the membrane was incubated in the solution of anti-mouse antibody conjugated with horseradish peroxidase (1 : 1000 dilution in PBS-Tween, Amersham-Pharmacia Biotech, UK) at 25 °C for 2 h. Luminescence was detected with an enhanced chemiluminescence detection kit (Amersham Pharmacia Biotech, UK).

Calcium signaling

HEK-293 cells expressing cfOR5269 were loaded with the Ca^{2+} sensitive fluorescent dye Fura-2 by incubation in Ringer's solution (140 mM NaCl, 1 mM $MgCl_2$, 1.8 mM $CaCl_2$, 5 mM KCl, 5 mM glucose, and 10 mM HEPES (pH 7.4)) containing 10 μM Fura-2/AM (Invitrogen, USA) at 37 °C for 30 min. Subsequently, Fura-2 loaded nanovesicles were produced from the cells as described above and collected *via* a centrifuge. The solution of produced nanovesicles was placed on a 96-well plate (Nunc, Germany) pre-coated with 0.1 mg mL^{-1} poly-D-lysine (PDL), and the fluorescence intensities from the nanovesicles were measured using a GENios Pro™ microplate reader (Tecan, Germany). A fluorescence emission at 510 nm was recorded with excitation alternating between 340 and 380 nm, and intracellular Ca^{2+} concentrations were determined from the ratio of fluorescence emissions (excitation at 340/380 nm).

Fabrication of OCBs

Fig. 1A shows a schematic diagram depicting the fabrication method of an OCB. At first, a CNT transistor was fabricated *via* the conventional photolithography method as reported previously.[22] In brief, methyl-terminated octadecyltrichlorosilane (OTS) molecules were patterned on a SiO_2 substrate *via* the conventional photolithography method to create non-polar regions. Then, the substrate was placed in CNT suspensions (0.05 mg mL^{-1} in dichlorobenzene) for ~10 s. In the suspensions, CNTs were selectively adsorbed onto the bare SiO_2 surface regions. And then, Ti (10 nm)/Au (20 nm) electrodes were fabricated *via* the photolithography process and covered with an insulating photoresist layer (DNR) to protect the contacts from the solution. In this method, CNTs randomly adhered on a bare SiO_2 region. We utilized CNTs comprised of both metallic and semiconducting ones. In this case, the transistors based on such CNTs did not turn off completely and were not suitable for integrated circuit applications. However, they exhibited a transconductance large enough for our sensor applications (Fig. S2 in the ESI†). The channel region of the CNT transistor was incubated with 0.1 mg mL^{-1} PDL solutions at 25 °C for 2 h to enhance the adsorption of nanovesicles. Then, a 1 μL droplet of nanovesicle solution was placed on the PDL-functionalized CNT channel region, and the device was incubated at 4 °C for 2 h. Since the shape of nanovesicles could be sustained only in a solution, OCBs should not be stored for over one day. We conducted sensing experiments just after the adsorption of olfactory nanovesicles onto CNT-FETs.

Electrical measurement for odorant sensing

For the sensing experiments, we prepared a polypropylene liquid well around our OCB chip to keep the liquid environments as

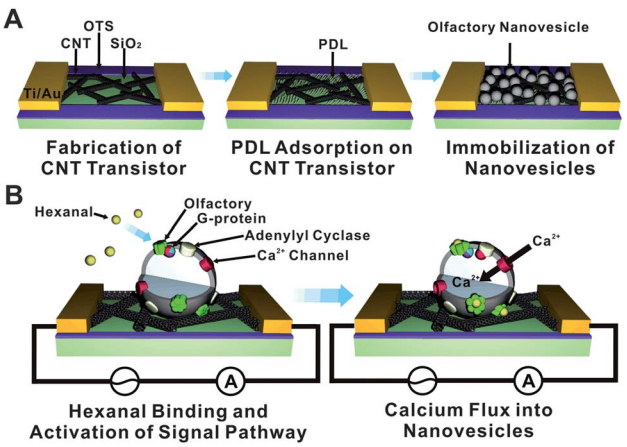

Fig. 1 OCB for the detection of hexanal. (A) Schematic diagram showing a method to prepare an OCB. A CNT-based transistor was coated with poly-D-lysine (PDL) for the stable adsorption of nanovesicles. Then, olfactory nanovesicles were immobilized on a CNT channel region in the transistor. (B) Schematic diagram showing the sensing mechanism for the detection of hexanal with an OCB. The binding of hexanal to ORs results in a Ca^{2+} influx into the nanovesicles through Ca^{2+} channels. Here, the accumulated Ca^{2+} ions inside the nanovesicles create a positive gate-potential in the vicinity of underlying CNTs, and the increased potential results in the decrease of conductance in the CNT channel.

reported previously.[27] Then, a 9 μL droplet of PBS containing Ca^{2+} (140 mM NaCl, 8 mM Na_2HPO_4, 1.5 mM KH_2PO_4, 0.5 mM $MgCl_2$, 1 mM $CaCl_2$) was placed on the OCB. The AC mode measurement method based on a lock-in amplifier was utilized to monitor the source–drain currents as sensor signals after applying the odorant solution with different concentrations. In this AC mode measurement scheme, an alternating voltage (30 mV, 31 Hz) was applied to the source and drain electrodes of an OCB by a function generator (Agilent Technologies, USA). A current through the electrodes was amplified by a low-noise current preamplifier (Stanford Research Systems, USA), and a lock-in amplifier (Stanford Research Systems, USA) was employed to measure the amplitude of the output signal of the preamplifier. This AC operation using a lock-in amplifier enabled the high-precision measurement of our sensor signals without being disturbed by environmental noises with different frequencies. Since the multiples or divisions of 60 Hz are common noise frequencies, we chose the prime-number frequency value of 31 Hz. Previously, a lock-in amplifier was utilized to measure the conductance of a FET sensor and detect biological and chemical species.[23] In this case, low operation frequencies such as 31 Hz were desirable so that the CNT-FET sensors can exhibit the characteristics close to that of DC mode operation.

Fig. 1B depicts the mechanism for the detection of hexanal using our OCB device. The binding of hexanal to ORs successively activated G proteins, adenylyl cyclases, and Ca^{2+} channels following the cAMP pathway in the nanovesicle.[13] The activation of Ca^{2+} channels generated an influx of Ca^{2+}, which increased the potential of the nanovesicle in the vicinity of CNTs. Since CNT channels exhibit a p-type behaviour under ambient conditions, the increased potential of the nearby nanovesicle resulted in the decrease of the CNT channel conductance. Note that, in the OCB device, the binding of odorant molecules onto olfactory receptors triggered the cAMP signal pathways in the nanovesicles, and the signal was measured by the CNT channels, which enabled the detection of target molecules with high sensitivity and high selectivity.

Preparation of odorants and spoiled milk

1 M solutions of hexanal, pentanal, heptanal, octanal, and hexanol (Sigma, USA) in dimethyl sulfoxide (DMSO, Sigma, USA) were first prepared, and diluted solutions (from 10 μM to 10 fM) were obtained by successive 1 : 10 dilutions in PBS containing Ca^{2+}. The prepared odorant solutions were stored at 4 °C until used. For the preparation of spoiled milk, milk was purchased at a local market and incubated at 25 °C for different time periods. Before experiments, the milk was diluted to 1 : 100 in PBS containing Ca^{2+}.

Vesicle fixation for scanning electron microscopy (SEM) imaging

Canine olfactory nanovesicles on CNT channel regions were fixed by incubation in 1% OsO_4 solution for 30 min. After the fixation of the nanovesicles, the substrate was washed with deionized water and then dehydrated in ethanol with increasing concentrations. Finally, the prepared substrate was dried in a critical point dryer (CPD 030, Balzers, Germany) and coated with Pt (10 nm) by a sputter (SCD 040, Balzers, Germany). The image of fixed nanovesicles on the CNT channel region was taken by SEM (JEOL, Japan) with a 30 kV accelerating voltage and a 13 000× magnification.

Result and discussion

Evaluation of the functionality of cfOR5269 in nanovesicles

Fig. 2A shows a Western blot image confirming the existence of cfOR5269 in nanovesicles. The bands of monomer, dimer, and multimer of cfOR5269 were observed. This result indicates that the active form of cfOR5269 proteins remained on the membrane of nanovesicles.

Fig. 2B shows the ratio of fluorescence emissions (excitation at 340/380 nm) from fura-2 loaded olfactory nanovesicles. Fura-2 is a fluorescent dye which binds to free Ca^{2+}. It is excited at 340 and 380 nm light, and the emissions at those wavelengths are correlated with the concentration of free Ca^{2+}. We immobilized fura-2 loaded nanovesicles on a 96-well plate. The nanovesicles were illuminated by an excitation beam with a wavelength alternating between 340 and 380 nm, and an emission at 510 nm was recorded. From the emission intensity, we calculated a fluorescence ratio. The fluorescence from nanovesicles without cfOR5269 did not change after the injection of 1 mM hexanal (red line). In the case of nanovesicles with cfOR5269, the fluorescence ratio increased after the injection of 1 mM hexanal (blue line), indicating the influx of Ca^{2+} into the nanovesicles. The results show that the cfOR5269 protein and Ca^{2+} signaling pathway were active in the nanovesicles.

Detection of hexanal with OCBs

Fig. 3A shows a SEM image of nanovesicles fixed on a CNT channel. The nanovesicles with a 100–200 nm diameter were immobilized on the CNT channel.

Fig. 3B shows the chemical structures of five different odorant molecules used in our experiment. Hexanal is the specific ligand

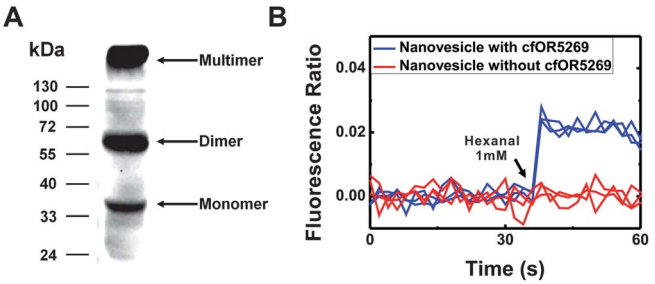

Fig. 2 Confirmation of the functionality of cfOR5269 in nanovesicles. (A) Western-blot image of cfOR5269 included in canine olfactory nanovesicles. The bands of cfOR5269 monomer, dimer and multimer indicate that the nanovesicles included the active form of cfOR5269 proteins. (B) Graph of the ratio of fluorescence emissions (excitation at 340/380 nm) from Fura-2-loaded olfactory nanovesicles. The ratio increased by the treatment of 1 mM hexanal only in nanovesicles with cfOR5269. The increase in the fluorescence ratio indicates that cfOR5269 in the nanovesicles maintained its original functionality in a cell membrane. Each line indicates a fluorescence ratio from nanovesicles in different wells of a 96-well plate.

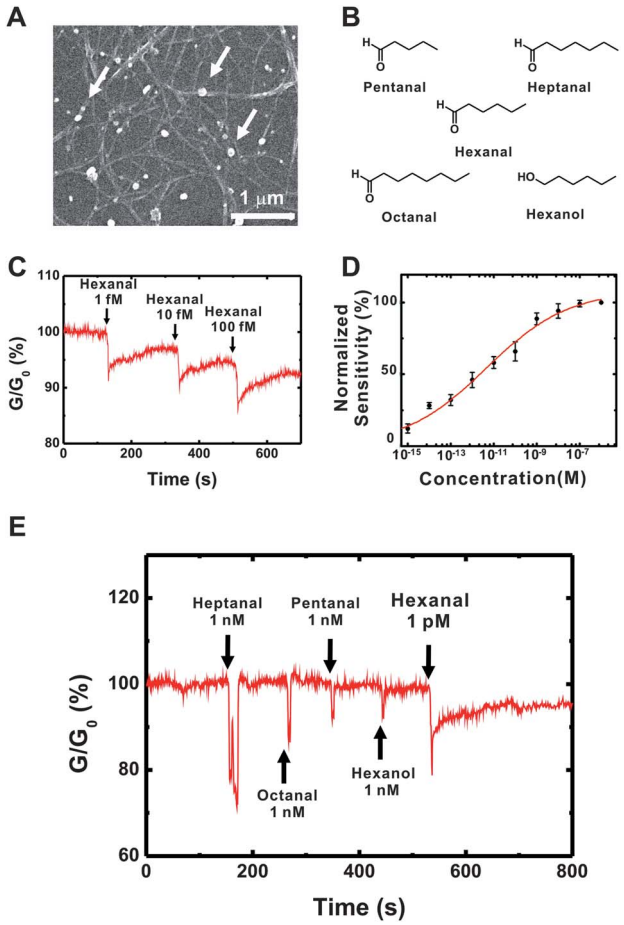

Fig. 3 Highly selective and sensitive detection of hexanal with OCB devices. (A) SEM image of nanovesicles immobilized on a CNT channel. The white arrows indicate the nanovesicles. (B) Chemical structures of various odorant molecules. Hexanal is the specific ligand of cfOR5269 protein. Note that the odorants have similar structures with slight differences in their alkyl chain length or functional groups. (C) Real-time conductance measurement data obtained from an OCB after the introduction of hexanal. The conductance decreased after the introduction of hexanal solution with a femtomolar concentration. (D) Response curve of OCBs ($n = 5$) to hexanal with different concentrations. The responses of OCBs were fitted to the Langmuir isotherm curve (red solid curve). (E) Real-time conductance measurement data obtained from an OCB after the injection of different odorants. The addition of 1 nM heptanal, octanal, pentanal and hexanol solutions had no effect on the conductance of the OCB, while the addition of 1 pM hexanal solution caused a sharp decrease in the conductance of the OCB.

of cfOR5269.[15] Note that the structures of the odorant molecules are very similar to each other except some minor differences such as their alkyl chain length or functional groups.

Fig. 3C shows real-time conductance measurement data obtained from an OCB after the introduction of hexanal with different concentrations. The OCB was first placed in PBS solution and the sample solutions were introduced. The OCB device exhibited a significant change in conductance with the injection of 1 fM hexanal solution. The results show the high sensitivity of our OCB devices.

We conducted the same experiment in Ca^{2+}-free environment (Fig. S3A in the ESI†). In this case, the addition of hexanal had no measurable effect on the conductance of the CNT channel of an OCB. This result shows that Ca^{2+} played a critical role in the change of the conductance of the CNT channel in the OCB device. Presumably, the binding of hexanal onto the cfOR5269 proteins on the nanovesicles triggered the Ca^{2+} signal pathway and, as a result, induced the influx of Ca^{2+} into the nanovesicles. The influx of Ca^{2+} resulted in the increase of potential in the vicinity of CNTs (Fig. 1B). Since CNT transistors exhibit p-type characteristics, the increased potential should have resulted in the reduction of conductance in the CNT channel.

Also, we conducted the same sensing experiment using nanovesicles without cfOR5269 (Fig. S3B in the ESI†). In this case, the conductance of the CNT channel of an OCB showed no observable response to the introduction of hexanal. This result also confirms the proposed response mechanism of our OCB devices as shown in Fig. 1B.

The response of OCB devices to different concentrations of hexanal solution can be analyzed using the Langmuir isotherm model (Fig. 3D). Since there were a finite number of OR molecules on the CNT channel of an OCB device, we can assume that hexanal was adsorbed onto cfOR5269 following the Langmuir isotherm.[24–28] In this case, the surface density C_S of hexanal bound to cfOR5269 on the CNT channel can be written as

$$C_S = \frac{C_{Smax} \times C}{1/K + C}$$

where C_{Smax}, C and K represent the surface density of cfOR5269 on the CNT channel, the concentration of hexanal in solution, and the equilibrium constant between hexanal and cfOR5269, respectively. In OCBs, the binding of hexanal to cfOR5269 induces the reduction of conductance in the underlying CNT channel. At a low concentration limit, we can approximate the sensor signal $|\Delta G/G_0|$ as $|\Delta G/G_0| \approx kC_S$, where k is a constant representing how sensitively OCBs would respond to the binding of hexanal (ESI†).[27] Thus, we can write $|\Delta G/G_0|$ as

$$|\Delta G/G_0| = \frac{kC_{Smax} \times C}{1/K + C}$$

When C is very large, $|\Delta G/G_0|$ saturates to the maximum value of kC_{Smax}. Thus, the measured conductance data can be normalized by its saturation value to calculate the normalized sensitivity N which can be written as

$$N = \frac{C}{1/K + C}$$

Previously, the responses of CNT-FETs to target molecules with various concentrations were analyzed by the Langmuir isotherm model, which allowed one to estimate the equilibrium binding constant K.[27,28]

Fig. 3D shows the normalized sensitivity of OCBs after the introduction of hexanal with various concentrations. Here, the conductance change of an OCB device was measured after the introduction of hexanal solutions with different concentrations, and the conductance change was normalized by its maximum to calculate the normalized sensitivity. We analyzed the responses of five OCBs to various concentrations of hexanal. The average values of normalized sensitivity are shown in Fig. 3D with error bars. The conductance change increased with the increasing concentration of hexanal. Finally, the

conductance change was almost saturated at 1 nM concentration. The data can be fitted to the Langmuir isotherm equation with the estimated equilibrium constant K of 5.0×10^{10} M^{-1}. Some research about the binding of hexanal to cfOR5269 was performed, but the equilibrium constant between hexanal and cfOR5269 has not been investigated before.[15,29] The result shows that our OCB platform may be utilized to study other OR proteins whose equilibrium constants are unknown.

Fig. 3E shows real-time conductance measurement data obtained from an OCB after the introduction of various odorants. The addition of 1 nM pentanal, heptanal, octanal, and hexanol did not affect the conductance of the OCB, while the addition of 1 pM hexanal caused a sharp decrease in the conductance. Note that the difference between those molecules is very minor. For example, the difference between hexanal and heptanal is just a *single carbon atom* in their alkane chains. This result shows our OCB devices could detect hexanal with a high selectivity.

Detection of hexanal in spoiled milk

Fig. 4 shows the conductance changes of OCBs after the introduction of 1 : 100 diluted spoiled milk to the OCBs. For the preparation of spoiled milk, fresh milk was incubated at 25 °C for 1–5 days. Since milk contains lots of lipid, hexanal can be produced by lipid oxidation during the incubation. An OCB device with nanovesicles without ORs did not respond to the addition of the spoiled milk (red line). On the other hand, an OCB with nanovesicles including ORs exhibited measurable changes in its conductance after the introduction of the milk rotten for 2 days, and the response increased with the increasing days of rotting (black line). Presumably, the hexanal in the spoiled milk bound to the ORs in the nanovesicles and, as a result, caused the conductance change of the CNT channel in the OCB (Fig. 1B). This result shows that OCBs may be applied to the fast on-site assessment of food quality.

We also performed a control experiment to find out the effect of other chemical species in the spoiled milk (Fig. S4 in the ESI†). We applied 1 : 100 diluted spoiled milk to a bare CNT sensor while monitoring the conductance of the sensor. The bare CNT channel did not respond to the introduction of the spoiled milk. This result also supports the proposed mechanism of our OCB devices (Fig. 1B).

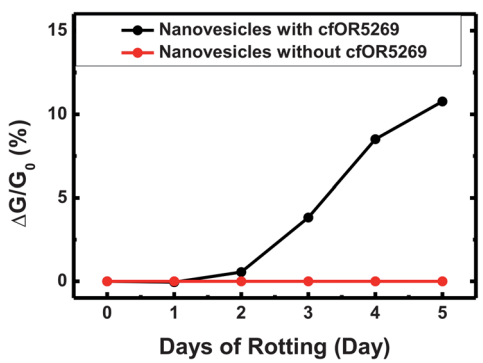

Fig. 4 Graph showing the conductance changes in OCBs after the introduction of spoiled milk. An OCB *with* nanovesicles including OR showed conductance changes after the introduction of spoiled milk (black line). No significant conductance change was observed in the case of an OCB with nanovesicles *without* OR (red line). These results indicate that the conductance changes were attributed to the binding of hexanal in the spoiled milk to cfOR5269 receptor molecules.

Conclusions

In summary, we developed a highly sensitive and selective olfactory-nanovesicle-fused bioelectronics sensor based on a canine olfactory nanovesicle–CNT hybrid structure for the detection of hexanal, an indicator of the oxidation of food. With this strategy, we could detect hexanal down to 1 fM concentration with excellent selectivity. Significantly, we detected hexanal in spoiled milk without any pretreatment processes. This result implies that OCBs can be applied for the easy and fast on-site assessment of food quality. Furthermore, by fabricating the arrays of sensors decorated with diverse olfactory receptors in a single chip, our platform could be extended toward a bioelectronic nose that mimics the natural olfactory system.[27] Also, since hexanal is known as a specific marker of lung cancer, our platform can be a useful tool for the screening of cancer diseases.[30]

Acknowledgements

This work was supported by the National Research Foundation of Korea (NRF) grant funded by the Korea government (MEST) (2011-0000390) and the Conversing Research Center Program (2011K000683). SH acknowledges the support from the NBIT program (2011-00240) and the NRF grant (2011-0020984). THP thanks the support from the NRF grant (no. 2011-0000331, 2011K000682, and 2011-0020984).

Notes and references

1 Y. D. Kim and C. V. Morr, *Int. Dairy J.*, 1996, **6**, 185–193.
2 M. G. Shin, S. H. Yoon, J. S. Rhee and T. W. Kwon, *J. Food Sci.*, 1986, **51**, 460–463.
3 S. Jadhav, D. K. Salunkhe and B. Singh, *Plant Cell Physiol.*, 1972, **13**, 449–459.
4 D. J. McClements and E. A. Decker, *J. Food Sci.*, 2000, **65**, 1270–1282.
5 W. H. Kunau and P. Dommes, *Eur. J. Biochem.*, 1978, **91**, 533–544.
6 H. W. Gardner, *Free Radical Biol. Med.*, 1989, **7**, 65–86.
7 F. Ulberth and D. Roubicek, *Int. Dairy J.*, 1995, **5**, 523–531.
8 F. Shahidi and R. B. Pegg, *ACS Symp. Ser.*, 1994, **558**, 256–279.
9 J. Lopez-Hernandez, A. Sanches-Silva, A. R. B. de Quiros and P. Paseiro-Losada, *J. Chromatogr., A*, 2004, **1046**, 75–81.
10 J. E. Haugen, F. Lundby, J. P. Wold and A. Veberg, *Sens. Actuators, B*, 2006, **116**, 78–84.
11 S. Maurizio, E. Sonia, M. GianFrancesco, S. Roberto, R. Ibanez, T. Agnese and U. Stefania, *Food Chem.*, 2009, **113**, 345–350.
12 X. B. Zou and J. W. Zhao, *Food Chem.*, 2008, **107**, 120–128.
13 S. Firestein, *Nature*, 2001, **413**, 211–218.
14 P. Mombaerts, *Science*, 1999, **286**, 707–711.
15 F. Gailibert, N. Benbernou, S. Tacher, S. Robin, M. Rakotomanga and F. Sfnger, *J. Hered.*, 2007, **98**, 500–505.
16 S. Panigrahi, S. Sankaran and S. Mallik, *Biosens. Bioelectron.*, 2011, **26**, 3103–3109.
17 T. H. Kim, S. H. Lee, J. Lee, H. S. Song, E. H. Oh, T. H. Park and S. Hong, *Adv. Mater.*, 2009, **21**, 91–94.
18 J. H. Sung, H. J. Ko and T. H. Park, *Biosens. Bioelectron.*, 2005, **20**, 1327–1332.
19 E. Pajot-Augy, J. M. Vidic, J. Grosclaude, M. A. Persuy, J. Aioun and R. Salesse, *Lab Chip*, 2006, **6**, 1026–1032.

20 P. Wang, Q. J. Liu, H. Cai, Y. Xu, Y. Li and R. Li, *Biosens. Bioelectron.*, 2006, **22**, 318–322.
21 H. Vogel, H. Pick, E. L. Schmid, A. P. Tairi, E. Ilegems and R. Hovius, *J. Am. Chem. Soc.*, 2005, **127**, 2908–2912.
22 M. Lee, J. Im, B. Y. Lee, S. Myung, J. Kang, L. Huang, Y. K. Kwon and S. Hong, *Nat. Nanotechnol.*, 2006, **1**, 66–71.
23 Y. Cui, Q. Wei, H. Park and C. M. Lieber, *Science*, 2001, **293**, 1289–1292.
24 N. J. Tao, E. S. Forzani, X. L. Li, P. M. Zhang, R. Zhang, I. Amlani, R. Tsui and L. A. Nagahara, *Small*, 2006, **2**, 1283–1291.
25 M. Lee, J. Lee, T. H. Kim, H. Lee, B. Y. Lee, J. Park, Y. M. Jhon, M. J. Seong and S. Hong, *Nanotechnology*, 2010, **21**, 055504.
26 T. H. Kim, H. S. Song, H. J. Jin, S. H. Lee, S. Namgung, U. K. Kim, T. H. Park and S. Hong, *Lab Chip*, 2011, **11**, 2262–2267.
27 B. Y. Lee, M. G. Sung, J. Lee, K. Y. Baik, Y. K. Kwon, M. S. Lee and S. Hong, *ACS Nano*, 2011, **5**, 4373–4379.
28 D. Son, S. Y. Park, B. Kim, J. T. Koh, T. H. Kim, S. An, D. Jang, G. T. Kim, W. Jhe and S. Hong, *ACS Nano*, 2011, **5**, 3888–3895.
29 F. Galibert, N. Benbernou, S. Robin, S. Tacher, M. Rimbault and M. Rakotomanga, *J. Hered.*, 2011, **102**, S47–S61.
30 X. M. Zhang, C. H. Deng and N. Li, *J. Chromatogr., B: Anal. Technol. Biomed. Life Sci.*, 2004, **808**, 269–277.

